Structure and interaction in protein solutions as studied by small-angle neutron scattering

S. Chodankar and V. K. Aswal
Solid State Physics Division, Bhabha Atomic Research Centre, Mumbai-400 085, India
(Received 30 March 2005; published 31 October 2005)

Small-angle neutron scattering (SANS) measurements have been performed to compare the effect of the salts KF, KCl, and KBr on crystallization in aqueous solution of lysozyme protein. It is found that the propensity of the salt to crystallize protein follows the Hoffmeister series (KF < KCl < KBr) with marked differences in the effect of these salts. In pure protein solution, lysozyme macromolecules are prolate ellipsoidal with semimajor and semiminor axes as 22 and 13.5 Å, respectively. SANS also gives that the effective (structural + counterion) charge (Z) on the protein as obtained by taking into account screened Coulomb interaction between the protein macromolecules is found to be much smaller than the structural charge. There is decrease in Z suggesting the higher counterion condensation on protein with the increase in the concentration. The counterion condensation seems to be responsible for the differences in the effect of different salts. It is also found that with the addition of salts, lysozyme macromolecules convert to dimers, and for the same salt concentration the comparative effect of different salts follows the Hoffmeister series. Time evolved measurements prior to and after the crystallization show that the protein solution mostly consists of monomers and dimers. Interestingly, higher-mers are not observed in these measurements as perhaps they are formed in very small numbers towards the process that leads to the crystallization. The time dependent data have been used to obtain the fraction of crystallization as a function of time.

DOI: 10.1103/PhysRevE.72.041931 PACS number(s): 87.14.Ee, 61.12.Ex, 87.15.Nn

I. INTRODUCTION

Protein macromolecules have a specific three-dimensional shape and charge on them, which regulates and controls the stability and biological functions of the protein. These macromolecules in solutions are known to be interacting due to the different interaction forces. Such interaction forces and structures of the macromolecules are at the heart of the living world, they are involved in controlling the macromolecular solubility and organization, in addition to governing fluid-fluid phase separation, crystal growth, or any separated protein phase. All these are controlled by the mechanism of molecular approach, reorientation, and incorporation. In such interactions the effective charge on the protein plays an important role. Only the stoichiometric values of the protein charge can be determined by titration experiments [1], since titration does not take into account the presence of ions that can condense on the charged macromolecules and change their net charge, as has been proved by the diffusion experiments [2]. The ability to control different protein phases can be done by deliberately tuning and obtaining the desirable changes in the interaction between protein-protein and protein additives by controlling the charge on the protein macromolecules.

A number of studies have been carried out on the behavior of protein in aqueous solution on addition of different additives (salt, alcohol, etc.) [3–14]. In particular, screening by background salt is known to play an important role in biology [15,16]. In the presence of salts, Hoffmeister effects [17–22] are common in biology, which emphasizes the choice of background salt in precipitating or controlling different phases in a protein solution. The charge neutralization on the macromolecules with the addition of salt depending on the charge on the macromolecule and ionic strength of the solution could bring the macromolecules closer and stacking them together could lead to the crystallization. It is believed that effectiveness of the salt for this purpose is governed by the counterion condensation that depends on the concentration and the nature of the salt [23,24]. The counterion located at short enough distances from the colloidal surface feels a strong electrostatic attraction compared with the thermal energy K_BT. These counterions are considered bound to or condensed on the colloid. The fact that counterion condensation on charged colloids depends on the hydrated size of the counterion will lead to the different effects of the salts having different sizes of counterions [25]. The condensation of charge determines the effective charge on the protein macromolecules and thus their structure and interaction.

Most of the studies on crystallization in protein solutions have been performed in the presence of electrolyte NaCl or KCl [3–9]. The variation of different counterions (e.g., KCl, KF, KBr) follows the sequence as given by the Hoffmeister series (KF < KCl < KBr). The relative effect of these counterions, however, will depend on the number of parameters such as surface charge density on the protein, number density of protein and counterions, size of the protein and counterions, etc. This makes it theoretically difficult to predict the actual effect of salt on the protein solution [26–28]. One of the simplest ways is to perform direct experiments and compare them. In this paper, we compare the effect of salts KF, KCl, and KBr on crystallization in aqueous solution of lysozyme protein. It is found that these salts show marked differences in their effects in protein solution. Small-angle neutron scattering (SANS) experiments have been carried out to compare the differences in the salt effect on protein crystallization in terms of structure and interaction present in the protein solutions.

II. EXPERIMENT

Hen egg white lysozyme (catalog no. L-6876) along with the salts KF, KCl, and KBr were purchased from Sigma and

were used as supplied without further purification. All the samples were prepared in D_2O. The use of D_2O instead of H_2O provides better contrast for hydrogenous samples in neutron scattering experiments. The lysozyme protein solutions were prepared about 12 h before the experiment so that the protein was completely dissolved without requiring any stirring or shaking which could cause denaturation of the protein. However, salts were added freshly at the start of each experiment. The phase diagram of protein crystallization was measured for fixed protein concentration (1 wt %) as a function of varying concentration of salts KF, KCl, and KBr. In these samples, depending on the salt and its concentration, the time period over which the crystallization had been monitored was 1–100 h. SANS studies on pure protein solutions were studied at different concentrations 1, 2, 5, and 10 wt %. The relative effect of different salts was performed at protein concentrations 1 and 5 wt % at various salt concentrations in the range 0–0.4 M. In one of these samples (i.e., 1-wt % protein+0.4-M KBr) that showed crystallization starting in about 1 h, SANS experiments were carried out to study evolution of structure during the process of crystallization every 10 min for about 20 h. The SANS experiments were carried out at Dhruva Reactor, Bhabha Atomic Research Centre, Mumbai [29] and at Swiss Spallation Neutron Source, SINQ, Paul Scherrer Institute, Switzerland [30]. In particular, the lower concentrations of protein and the time resolve measurements were performed at the SINQ SANS instrument because of the high signal to background ratio of this instrument. The data were collected in the Q range of 0.010–0.35 $Å^{-1}$. The temperature for all the above measurements was kept fixed at 30 °C. The measured SANS data were corrected and normalized to a cross-sectional unit using standard procedures.

III. SANS ANALYSIS

In small-angle neutron scattering one measures the coherent differential scattering cross section $(d\Sigma/d\Omega)$ per unit volume. For a system of monodisperse interacting protein macromolecules, $d\Sigma/d\Omega$ can be expressed as [31]

$$\frac{d\Sigma}{d\Omega} = n(\rho_m - \rho_s)^2 V^2 \{\langle F^2(Q)\rangle + \langle F(Q)\rangle^2 [S(Q) - 1]\} + B, \tag{1}$$

where n denotes the number density of the protein macromolecules, ρ_m and ρ_s are, respectively, the scattering length densities of the protein macromolecules and the solvent, and V is the volume of the protein macromolecule. $F(Q)$ is the single particle form factor and $S(Q)$ is the interparticle structure factor. B is a constant term that represents the incoherent scattering background, which is mainly due to hydrogen in the sample. The single particle form factor has been calculated by treating the protein macromolecules as prolate ellipsoidal. For such an ellipsoidal particle

$$\langle F^2(Q)\rangle = \int_0^1 [F(Q,\mu)^2 d\mu], \tag{2}$$

$$\langle F(Q)\rangle^2 = \left[\int_0^1 F(Q,\mu) d\mu\right]^2, \tag{3}$$

$$F(Q,\mu) = \frac{3(\sin x - x\cos x)}{x^3}, \tag{4}$$

$$x = Q[a^2\mu^2 + b^2(1-\mu^2)]^{1/2}, \tag{5}$$

where a and b are, respectively, the semimajor and semiminor axes of the ellipsoidal protein macromolecules and μ is the cosine of the angle between the directions of a and the wave vector transfer Q.

In general, charged colloidal solutions show a correlation peak in the SANS distribution. The peak arises because of the interparticle structure factor $S(Q)$ and indicates the presence of electrostatic interaction between the colloids. $S(Q)$ specifies the correlation between the centers of different particles and it is the Fourier transform of the radial distribution function $g(r)$ for the mass centers of the particles. We have calculated $S(Q)$ as derived by Hayter and Penfold from the Ornstein-Zernike equation and using the mean spherical approximation [32]. The protein macromolecules are assumed to be a rigid equivalent sphere of diameter $\sigma=2(ab^2)^{1/3}$ interacting through a screened Coulomb potential.

Equation (1) for noninteracting particles [i.e., $S(Q)\sim 1$] is given by

$$\frac{d\Sigma}{d\Omega} = n(\rho_m - \rho_s)^2 V^2 \langle F^2(Q)\rangle + B. \tag{6}$$

The addition of salts in protein solutions leads to the formation of dimers and higher-mers towards the protein crystallization. The form factor for a system consisting of n-mers is given by [33]

$$\langle F^2(Q)\rangle_n = \sum_{i,j=1}^{n} F_i(Q) F_j(Q) \frac{\sin Qd_{ij}}{Qd_{ij}}, \tag{7}$$

where d_{ij} is the distance between the centers of the ith and jth monomers.

In the case of dilute protein solution and in the presence of salts, a protein solution consisting of monomers and dimers, Eq. (6) in combination with Eq. (7), can be written as

$$\frac{d\Sigma}{d\Omega} = n(\rho_m - \rho_s)^2 V^2 [(1-f)\langle F^2(Q)\rangle + 0.5f\langle F^2(Q)\rangle_2]. \tag{8}$$

Here f is the fraction of monomers that form the dimers. The form factor for the dimers $\langle F^2(Q)\rangle_2$ is given as

$$\langle F^2(Q)\rangle_2 = 2\langle F^2(Q)\rangle \left[1 + \frac{\sin Qd_{12}}{Qd_{12}}\right]. \tag{9}$$

The dimensions of the protein macromolecule and the effective charge on the protein in pure protein solutions have been determined from the analysis. The semimajor axis (a), semiminor axis ($b=c$), and the effective charge (Z) are the parameters in analyzing the SANS data. The SANS analysis in the presence of salts were carried out for low protein concentrations to make use of Eq. (6). Data were fitted assuming

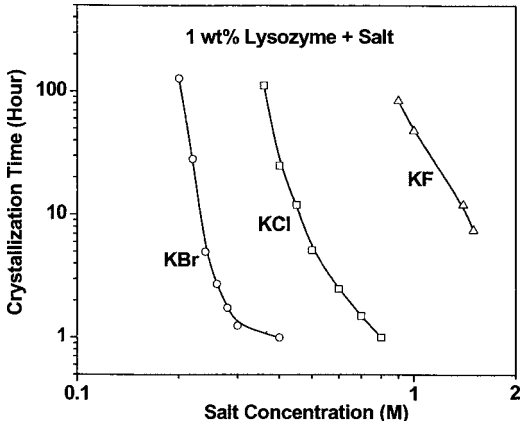

FIG. 1. Phase diagram of crystallization of 1-wt % lysozyme in the presence of salts KF, KCl, and KBr.

the salt induces the formation of dimers and higher-mers. However, it is seen that the protein solution in the presence of salts only consists of monomers and dimers. Throughout the data analysis, the corrections were made for instrumental smearing. For each instrumental setting the scattering profiles as given by Eqs. (1) or (6) were smeared by the appropriate resolution function to compare with the measure data [29]. The parameters in the analysis were optimized by means of a nonlinear least-square fitting program and the errors on the parameters were calculated by the standard method [34].

IV. RESULTS AND DISCUSSION

Figure 1 shows the phase diagram of the crystallization of 1 wt % lysozyme protein solution as a function of varying concentration of salts KF, KCl, and KBr. The data points in the phase diagram represent the times at which the first appearance of crystallization in protein solutions were visually observed. It is seen, as expected, that the comparative effects of these salts to induce crystallization follows the Hoffmeister series (KF < KCl < KBr) [17–22]. However, it is most important to note that the effects of these salts are markedly

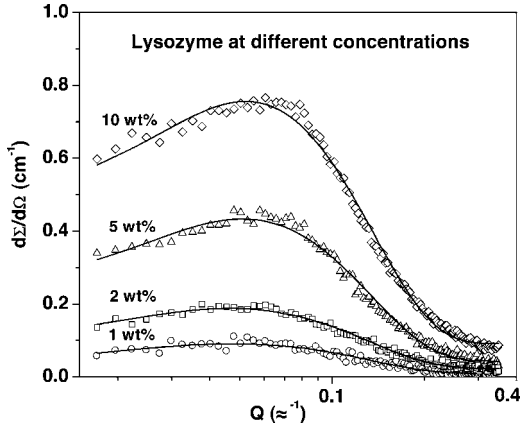

FIG. 2. SANS data on aqueous lysozyme solution at different protein concentrations.

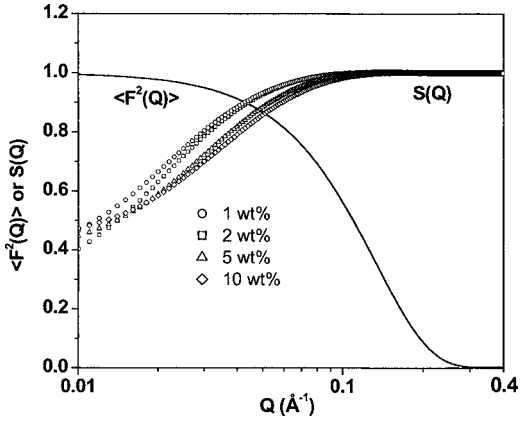

FIG. 3. The calculated $\langle F^2(Q)\rangle$ and $S(Q)$ for different concentrations of lysozyme.

different. For example, while the addition of 0.4-M KBr produces crystallization as early as about 1 h, it takes about 25 h with KCl and does not occur even up to two weeks for KF for the similar concentration of salts. In the presence of a given salt, there is an asymptotic time dependence of occurrence of crystallization in the low concentration regime of the salt and the propensity of the crystal formation increases with the increase in the salt concentration. Figure 1 thus shows the importance of nature and the concentration of the salts in inducing the crystallization of protein solution.

SANS data on a pure aqueous solution of lysozyme protein at concentrations of 1, 2, 5, and 10 wt % are shown in Fig. 2. All the data show a correlation peak, which is an indication of the interacting charge protein macromolecules in the solution. The solid lines in Fig. 2 are the fitted curves using Eq. (1). Figure 3 shows the calculated $\langle F^2(Q)\rangle$ and $S(Q)$ in the protein solutions. This suggests that the peak position in scattering data (Fig. 2) does not change with the variation in concentration because of the weak concentration dependence of $S(Q)$. The parameters of the SANS analysis

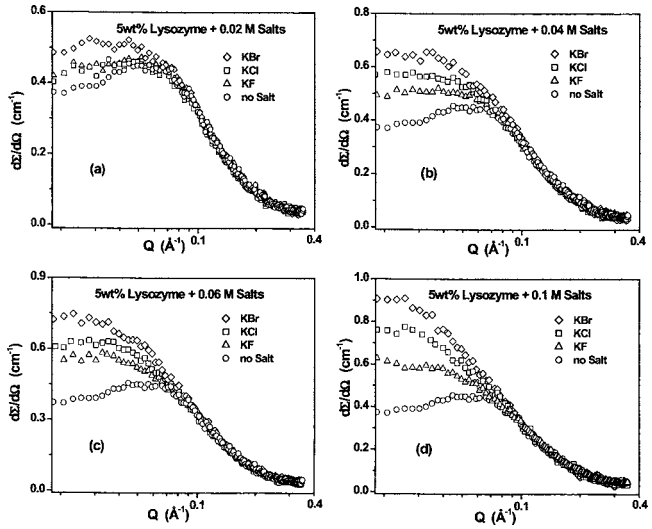

FIG. 4. SANS data (a)–(d) correspond to 5-wt % lysozyme in the presence of salts at concentrations 0.02, 0.04, 0.06, and 0.1 M, respectively.

TABLE I. The parameters of lysozyme macromolecule at different protein concentrations in aqueous solution.

	Size dimensions		
Concentration (wt %)	Semimajor axis a (Å)	Semiminor axis $b=c$ (Å)	Effective charge Z (e)
1	22±2.5	13.5±1.0	2.8±1.0
2	22±1.5	13.5±0.5	1.9±0.8
5	22±1.0	13.5±0.5	1.6±0.6
10	22±1.0	13.5±0.5	1.3±0.4

are given in Table I. It is found that lysozyme protein macromolecules are prolate ellipsoidal with dimensions of semimajor and semiminor axes as 22.0 and 13.5 Å, respectively. These results are in agreement with the values reported earlier [5,13,35]. Table I shows that the effective charge decreases with the increase in protein concentration and it is found to be much smaller than that of the structural charge ($+7e$) on the protein. It may be noted that in SANS one measures the effective charge, which is the structural charge surrounded by the condensed counterions [36–39]. That the effective charge decreases with the concentration is an indication of increase in the counterion condensation around the charged macromolecule. Similar results of concentration dependence of counterion condensation have also been observed in charge colloidal solutions such as micelles [40,41]. The fact that the SANS measures the scattering intensity to the absolute scale of cross section can be used to determine the contrast term $(\rho_m-\rho_s)^2$ in Eq. (1). This has been used to see the hydration of lysozyme macromolecules as connected to the scattering length of the macromolecule (ρ_m). It is found that 55±5-vol % water of hydration to the lysozyme scales to the measured scattering cross section.

Figures 4(a)–4(d) show the SANS data of 5-wt % lysozyme in the presence of different salts (KF, KCl, and KBr) at concentrations 0.02, 0.04, 0.06, and 0.1 M, respectively. It is observed that on addition of salts, the correlation peak broadens along with a shift in the peak position to the lower Q region. The broadening and shift in the peak position increases with an increase in the salt concentration. The effect of different salts on the changes in the SANS data for a given concentration follows the Hoffmeister series (KF $<$KCl$<$KBr). The shifting and broadening of the peak in SANS data on addition of salts is an indication of charge neutralization on the protein and that leads to the agglomeration of protein macromolecules [36–41]. This is supported by the fact that the SANS data do not fit Eq. (1) which assumes the protein solution consists of individual macromolecules interacting through the screened Coulomb interaction. The qualitative features of SANS data [Figs. 4(a)–4(d)] are in accordance with those governed by counterion condensation [38,39]. The counterion condensation decides the charge neutralization, which increases with the salt concentration, and for a given counterion it is more when the hydrated size of counterions is less. It is also believed that short-range attraction becomes important with the screening of electrostatic repulsion in the presence of salts [42–46]. The agglomeration in protein solutions on addition of salts makes it difficult to determine quantitatively the role of effective potential, due to complications in the calculation of $S(Q)$ for different sizes of aggregates. However, it is possible with the dilute protein solutions [$S(Q)\sim 1$] to determine the agglomeration in the presence of salts as described below.

Figure 5 shows the SANS data for 1-wt % lysozyme in the presence of KCl at concentrations 0.1, 0.2, and 0.4 M. The low concentration of lysozyme and high concentrations of salt have been used to make sure that data can be analyzed taking $S(Q)\sim 1$. The data are fitted for $\langle F^2(Q)\rangle$ using Eq. (6) considering that the protein solution consists of aggregates of

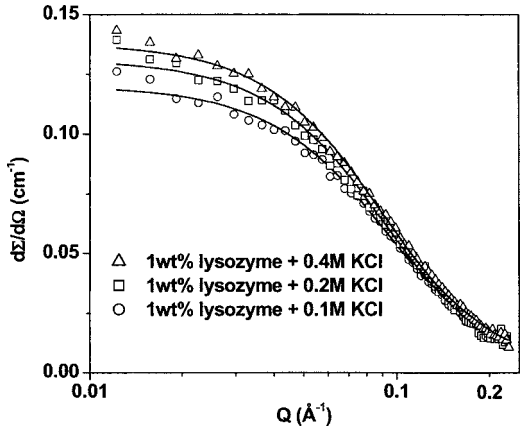

FIG. 5. SANS data on 1-wt % lysozyme in the presence of KCl at 0.1, 0.2, and 0.4 M.

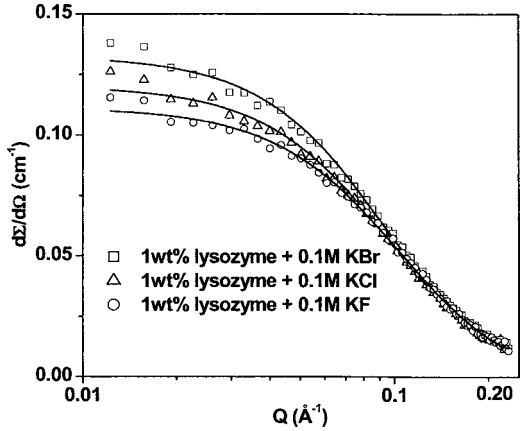

FIG. 6. SANS data on 1-wt % lysozyme on fixed concentration (0.1 M) of salts KBr, KCl, and KF.

TABLE II. The fraction of monomers converting to dimers on 1 wt % lysozyme in the presence of salts.

Protein sample	Dimer fraction
1 wt % lysozyme+0.1-M KCl	0.32±0.04
1 wt % lysozyme+0.2-M KCl	0.44±0.04
1 wt % lysozyme+0.4-M KCl	0.56±0.06
1 wt % lysozyme+0.1-M KBr	0.66±0.08
1 wt % lysozyme+0.1-M KF	0.22±0.04

different sizes (i.e., monomers, dimers, and higher-mers). The analysis suggests that the protein solution mostly consists of monomers and dimers. The parameters of the analysis are given in Table II. It is seen that the dimer fraction increases with the increase in the salt concentration. The comparison of salts KF, KCl, and KBr on dimer formation is shown in Fig. 6. The data are shown for fixed lysozyme (1 wt %) and salt (0.1 M) concentrations. The analysis (Table II) shows that the propensity to form dimers follows the Hoffmeister series that KBr is much more effective as compared to KCl and KF.

Figure 7 shows the SANS data prior to crystallization on one of the samples (1-wt % lysozyme+0.4-M KBr) in the phase diagram of Fig. 1. The formation of small crystals in this sample starts in about 1 h. The SANS data in Fig. 7 were recorded at every 10 min. It is interesting to note that the data do not show any significant changes up to 1 h when the crystallization has started in the protein solution. This observation suggests that protein solution at crystallization still mostly consists of monomers and dimers and the fraction of monomers and dimers that leads to crystallization is very small. Figure 8 shows the SANS data to study the rate of crystallization in 1-wt % lysozyme+0.4-M KBr over a long time until the crystallization in the solution almost saturates. The data in Fig. 8 were measured in an interval of $\frac{1}{2}$ h starting from freshly prepared sample up to 20 h. Figure 8 shows that the scattering intensity decreases with time only after some time of the start of crystallization. However, the features of the scattering profile remain the same. The scaling of the data after correcting for the incoherent background from the sample measured at 0, 2, 4, 8, 12, 16, and 20 h is shown in the inset of Fig. 8. The fact that the functionality of the scattering profile does not change as a function of time suggests that even after a long time after the start of crystallization, the protein solution mostly consists of monomers and dimers. Higher-mers that lead to crystallization are not observed in the solution. This is possible if the higher-mers including nucleated structure are formed in very small numbers (not sensitive to the SANS measurement) in the process towards the crystallization. Figure 9 gives the crystallization fraction as a function of time as obtained from the scaling of SANS data in Fig. 8. It is seen even after some time (1–2 h) after when crystallization has started (~1 h) that the crystal concentration is very small. Further, as time progresses, crystallization increases linearly (~2–10 h) and the formation of crystals almost saturates at longer times. The available fraction of monomers and dimers may not be enough at longer times to sustain the crystallization.

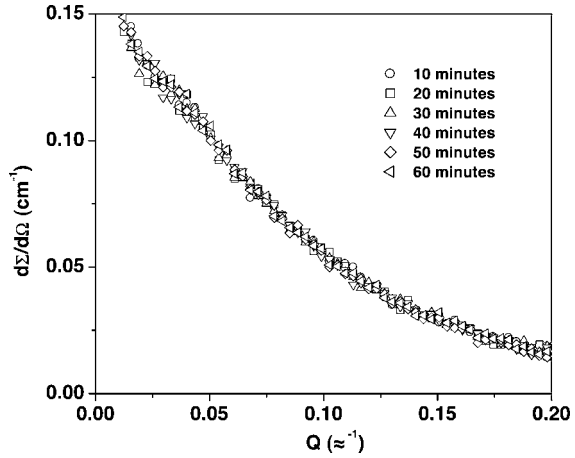

FIG. 7. Time evolved SANS data prior to crystallization on 1-wt % lysozyme in the presence of 0.4-M KBr. The data were taken for every 10 min up to 1 h until the crystallization occurs.

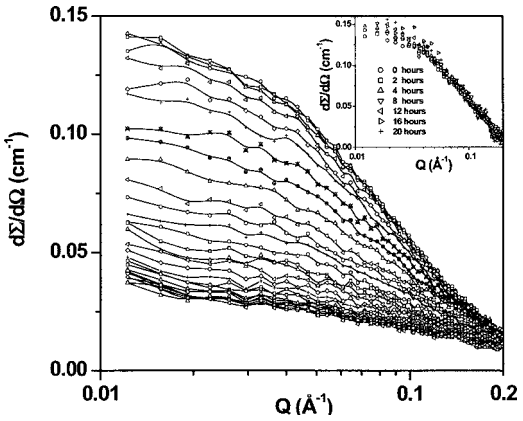

FIG. 8. Time evolved SANS data prior to and after crystallization on 1-wt % lysozyme in the presence of 0.4-M KBr. The data were taken in $\frac{1}{2}$-h intervals up to 20 h. The different data profiles correspond to a decrease in scattering intensity with the increase in time.

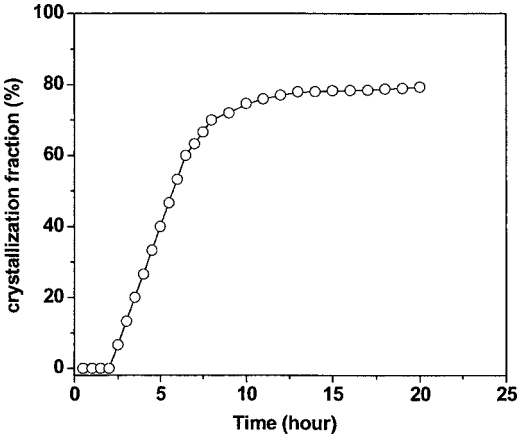

FIG. 9. The rate of crystallization as a function of time on 1-wt % lysozyme in the presence of 0.4-M KBr.

V. CONCLUSION

SANS has been used to compare the effect of the salts KF, KCl, and KBr on crystallization in aqueous solution of lysozyme protein. The propensity of the salts to crystallize protein follows the Hoffmeister series (KF < KCl < KBr) with marked differences in the effect of these salts. For example, while the addition of 0.4-M KBr produces crystallization as early as in about 1 h, it takes about 25 h with KCl and does not occur even up to two weeks for KF for a similar concentration of salts. The charge neutralization as a result of counterion condensation seems to be responsible for the differences in the effect of the above salts. Time evolved measurements prior to crystallization show that the protein solution mostly consists of monomers and dimers and the fraction of monomers and dimers that leads to crystallization is very small. It is also found that even after the start of crystallization to the saturation, the solution mostly consists of monomers and dimers. Higher-mers are not observed as perhaps they are formed in very small numbers towards the process that leads to crystallization.

ACKNOWLEDGMENTS

We thank the Swiss Spallation Neutron Source at the Paul Scherrer Institut (PSI), Switzerland, for a beam time for performing a part of SANS work in this paper. We also thank J. Kohlbrecher for his support and useful discussion during the experiments at PSI.

[1] J. G. Albright, O. Annunziata, D. G. Miller, L. Paduano, and A. J. Pearlstein, J. Am. Chem. Soc. **121**, 3256 (1999).
[2] C. Tanford and M. L. Wagner, J. Am. Chem. Soc. **76**, 3331 (1954).
[3] H. B. Stuhrmann and H. Fuess, Acta Crystallogr., Sect. A: Cryst. Phys., Diffr., Theor. Gen. Crystallogr. **A32**, 67 (1976).
[4] M. Madeleine, M. Riès-Kautt, and A. F. Ducruix, J. Cryst. Growth **110**, 20 (1991).
[5] R. Giordano, A. Grasso, J. Teixeira, and U. Wanderlingin, Physica B **180 & 181**, 762 (1992).
[6] N. Niimura, Y. Minezaki, M. Ataka, and T. Katsura, J. Cryst. Growth **137**, 671 (1994).
[7] N. Niimura, Y. Minezaki, M. Ataka, and T. Katsura, J. Cryst. Growth **154**, 136 (1995).
[8] N. Niimura, Y. Minezaki, I. Tanaka, S. Fujiwara, and M. Ataka, J. Cryst. Growth **200**, 265 (1999).
[9] I. Broutin, M. Madeleine, M. Riès-Kautt, and A. Ducruix, J. Appl. Crystallogr. **28**, 614 (1995).
[10] S. Tanaka, M. Yamamoto, K. Kawashima, K. Ito, R. Hayakawa, and M. Ataka, J. Cryst. Growth **168**, 44 (1996).
[11] R. A. Curtis, J. M. Prausnitz, and H. W. Blanch, Biotechnol. Bioeng. **57**, 11 (1998).
[12] R. A. Curtis, J. Ulrich, A. Montaser, J. M. Prausnitz, and H. W. Blanch, Biotechnol. Bioeng. **79**, 367 (2002).
[13] O. D. Velev, E. W. Kaler, and A. M. Lenhoff, Biophys. J. **75**, 2682 (1998).
[14] J. J. Grigsby, H. W. Blanch, and J. M. Prausnitz, Biophys. Chem. **91**, 231 (2001).
[15] J. N. Israelachvili, *Intermolecular and Surface Forces* (Academic, London, 1990), 2nd ed.
[16] R. J. Hunter, *Foundations of Colloid Science* (Oxford University, New York, 1989).
[17] P. H. Von Hippel and T. Schleich, *Structure and Stability of Biological Macromolecules* (Marcel Dekker, New York, 1969).
[18] M. Riès-Kautt, in *Protein Crystallization: Techniques, Strategies, and Tips*, edited by T. M. Bergfors (International University Line, La Jolla, 1999).
[19] R. L. Baldwin, Biophys. J. **71**, 2056 (1996).
[20] M. Bostrom, D. R. M. Williams, P. R. Stewart, and B. W. Ninham, Phys. Rev. E **68**, 041902 (2003).
[21] M. Bostrom, D. R. M. Williams, and B. W. Ninham, Phys. Rev. Lett. **87**, 168103 (2001).
[22] M. Bostrom, D. R. M. Williams, and B. W. Ninham, J. Phys. Chem. B **106**, 7908 (2002).
[23] F. Oosawa, *Polyelectrolytes* (Dekker, New York, 1971).
[24] G. S. Manning, J. Chem. Phys. **51**, 924 (1969).
[25] V. K. Aswal and P. S. Goyal, Phys. Rev. E **61**, 2947 (2000).
[26] G. V. Ramanathan, J. Chem. Phys. **88**, 3887 (1988).
[27] I. Borukhov and D. Andelman, Phys. Rev. Lett. **79**, 435 (1997).
[28] L. Belloni, Colloids Surf., A **140**, 227 (1998).
[29] V. K. Aswal and P. S. Goyal, Curr. Sci. **79**, 947 (2000).
[30] J. Kohlbrecher and W. Wagner, J. Appl. Crystallogr. **33**, 804 (2000).
[31] J. B. Hayter and J. Penfold, Colloid Polym. Sci. **261**, 1022 (1983).
[32] J. B. Hayter and J. Penfold, Mol. Phys. **42**, 109 (1981).
[33] J. S. Pedersen, Adv. Colloid Interface Sci. **70**, 171 (1997).
[34] P. R. Bevington, *Data Reduction and Error Analysis for Physical Sciences* (McGraw-Hill, New York, 1969).
[35] E. Seth and V. K. Aswal, J. Macromol. Sci., Phys. **B41**, 77 (2002).
[36] D. Bendedouch and S. H. Chen, J. Phys. Chem. **88**, 648 (1984).
[37] M. Bergstrom and J. S. Pedersen, Phys. Chem. Chem. Phys. **1**, 4437 (1999).
[38] V. K. Aswal and P. S. Goyal, Chem. Phys. Lett. **364**, 44 (2002).
[39] V. K. Aswal and P. S. Goyal, Phys. Rev. E **67**, 051401 (2003).
[40] S. S. Berr, J. Phys. Chem. **91**, 4760 (1987).
[41] V. K. Aswal and P. S. Goyal, Chem. Phys. Lett. **357**, 491 (2002).
[42] M. Malfois, F. Bonneté, L. Belloni, and A. Tardieu, J. Chem. Phys. **105**, 3290 (1996).
[43] A. Tardieu, A. Le Verge, M. Malfois, F. Bonneté, S. Finet, M. Riès-Kautt, and L. Belloni, J. Cryst. Growth **196**, 193 (1999).
[44] R. Piazza, Curr. Opin. Colloid Interface Sci. **5**, 38 (2000).
[45] G. Foffi, G. D. McCullagh, A. Lawlor, E. Zaccarelli, K. A. Dawson, F. Sciortino, P. Tartaglia, D. Pini, and G. Stell, Phys. Rev. E **65**, 031407 (2002).
[46] A. Stradner, H. Sedgwick, F. Cardinaux, W. C. K. Poon, S. U. Egelhaaf, and P. Schurtenberger, Nature (London) **32**, 492 (2004).